Biomaterials 31 (2010) 8419–8425

Contents lists available at ScienceDirect

Biomaterials

journal homepage: www.elsevier.com/locate/biomaterials

Neutron capture nuclei-containing carbon nanoparticles for destruction of cancer cells

Kuo Chu Hwang [a,*], Po Dong Lai [a], Chi-Shiun Chiang [b], Pei-Jen Wang [c], Chiun-Jye Yuan [d]

[a] Department of Chemistry, National Tsing Hua University, Hsinchu 30043, Taiwan, ROC
[b] Department of Biomedical Engineering and Environmental Sciences, National Tsing Hua University, Hsinchu 30043, Taiwan, ROC
[c] Department of Power Mechanical Engineering, National Tsing Hua University, Hsinchu 30043, Taiwan, ROC
[d] Department of Biological Science and Technology, National Chiao-Tung University, Hsinchu 30043, Taiwan, ROC

ARTICLE INFO

Article history:
Received 23 June 2010
Accepted 13 July 2010
Available online 10 August 2010

Keywords:
Nanoparticles
Biocompatibility
Cell viability
Cell proliferation
Drug delivery

ABSTRACT

HeLa cells were incubated with neutron capture nuclei (boron-10 and gadolinium)-containing carbon nanoparticles, followed by irradiation of slow thermal neutron beam. Under a neutron flux of 6×10^{11} n/cm^2 (or 10 min irradiation at a neutron flux of 1×10^9 n/cm^2 s), the percentages of acute cell death at 8 h after irradiation are 52, 55, and 28% for HeLa cells fed with BCo@CNPs, GdCo@CNPs, and Co@CNPs, respectively. The proliferation capability of the survived HeLa cells was also found to be significantly suppressed. At 48 h after neutron irradiation, the cell viability further decreases to ~35 ± 5% as compared to the control set receiving the same amount of neutron irradiation dose but in the absence of carbon nanoparticles. This work demonstrates "proof-of-concept" examples of neutron capture therapy using ^{10}B-, ^{157}Gd-, and ^{59}Co-containing carbon nanoparticles for effective destruction of cancer cells. It will also be reported the preparation and surface functionalization of boron or gadolinium doped core–shell cobalt/carbon nanoparticles (BCo@CNPs, GdCo@CNPs and Co@CNPs) using a modified DC pulsed arc discharge method, and their characterization by various spectroscopic measurements, including TEM, XRD, SQUID, FT-IR, etc. Tumor cell targeting ability was introduced by surface modification of these carbon nanoparticles with folate moieties.

1. Introduction

The concept of using boron neutron capture therapy (BNCT) for cancer treatments was first proposed in 1936 by Locher [1]. The principal concept is to treat tumors with molecules containing elements of very high neutron capture cross-section, such as, ^{10}B, ^{157}Gd, etc. Upon capture of slow thermal neutrons, ^{10}B atom was transformed into radioactive ^{11}B which then immediately decompose and release highly energetic alpha and recoiling ^{7}Li particles to destroy nearby cancer cells. The mean free path of high energy α and ^{7}Li particles are in the range of ~10 μm which is smaller than the average size (10–15 μm) of cells [2]. Therefore, the high energy α and recoiling ^{7}Li particles will only destroy the cells where the ^{10}B-containing species are located, and will not causes damages to other long-distanced normal cells. The neutron absorption cross-sections of various elements are dramatically different, for example, C(0.0034 b, 1 b = 1×10^{-24} cm^2), H(0.33 b), O(1.8×10^{-4} b), N(1.8 b), P(0.18 b), Na (0.43 b), ^{10}B(3538 b), ^{155}Gd(61000 b), ^{157}Gd(255000 b), ^{59}Co(1900 b), etc [3]. In human bodies, the neutron absorption cross-sections of major elements, such as, H, O, and C, are 4–8 orders smaller than that of ^{10}B. Therefore, as long as there is a sufficient amount of ^{10}B elements accumulated in a tumor site, thermal neutron irradiation will cause death of tumor cells, but leave the surrounding normal cells unharmed. Normal brain tissue has a so-called "brain–blood barrier" to restrict diffusion of large and hydrophilic molecules to enter the cerebrospinal fluid in the central nervous system. Unlike the normal brain tissues, brain tumors are much more permeable to medicinal molecules than normal brain tissue. The brain tumor, glioblastoma multiforme (GBM), grows rapidly, and is poorly responsive to the conventional therapeutic treatments. Patients with GBM have a quite short average lifespan of 6–9 months after diagnosis. BNCT brings a new hope for treatment of malignant brain tumors. In the literature, several generations of ^{10}B-containing drugs have been developed and their efficacies examined clinically. The first generation of ^{10}B-delivering molecules includes sodium borate, boric acid and derivatives. These first generation boron-containing molecules do not have the tumor targeting ability, and cannot reach a sufficiently high tumor-to-blood boron ratio for effective neutron capture therapy efficacy. Consequently, their clinical treatments of malignant tumors have been proven failure [4]. In the development of the second generation

* Corresponding author. Tel./fax: +886 3572 4810.
E-mail address: kchwang@mx.nthu.edu.tw (K.C. Hwang).

0142-9612/$ – see front matter © 2010 Elsevier Ltd. All rights reserved.
doi:10.1016/j.biomaterials.2010.07.057

of BNCT agents, emphasis was put on the ability of molecules being able to be selectively up taken by tumor cells, or have tumor-seeking properties. Well known molecules include mercaptoundecahydrododecaborane (BSH), 4-dihydroxyboryl phenylalanine (BPA), etc [5–7]. Up to date, the use of BNCT agents for curing of cancers has achieved only very limited success [8–13]. In recent years, many newly designed BNCT reagents have been prepared, including borane-attached porphyrin [14], borate–lipid liposomes [15,16], etc. One of the major obstacles encountered in these previous studies is that it is difficult to deliver enough doses of ^{10}B-containing molecules into tumor cells, while still keep a high tumor-to-blood boron ratio.

Theoretical simulation using Monte Carlo-based treatment planning system (INEEL) program shows that the ^{10}B atoms dose required for effective destruction of cancer cells is 20–35 μg per gram tumor cells or ~10^9 ^{10}B atoms in each tumor cell [16]. For ^{157}Gd-containing medicine, the effective dose is 50–200 μg per gram tumor cells. Currently, there is lack of any ^{10}B- or ^{157}Gd-containing molecules which meet the above requirement [8–13]. Since the amount of ^{10}B- or ^{157}Gd-containing molecules within a tumor cell cannot reach the effective dosage, the death rate of tumor cells, upon neutron irradiation, is usually very modest. Previously, single walled carbon nanotubes have been widely used as biological cargoes for transportation of biologically active molecules into cells [17–19]. For the purpose of BNCT, substituted C_2B_{10} carborane cage was chemically attached onto SWCNTs [10]. Animal model study showed that the carborane-SWNT complex can selectively accumulate in the EMT6 tumor cells in mice with a maximum concentration of 22.8 μg boron per gram tissue. The cytotoxicity of the carborane–SWCNT complex and the neutron irradiation therapeutic effects, however, were not reported. In another study, ball-milled non-magnetic B_4C particles were surface modified with various functional groups and fed to B16 F10 malignant melanoma cells [11]. After neutron irradiation, the proliferation capability, by measuring ^3H-thymidine incorporation, of B16 F10 malignant melanoma cells was found to be significantly inhibited. Information regarding the cytotoxicity of B_4C particles and neutron irradiation induced cell death, however, was not reported either.

To realize the effects of BNCT, several challenges have to be overcome: (a) the local concentration of ^{10}B in a tumor has to be as high as possible, close to or higher than 20–30 μg/g cells (or ~10^9 boron atoms per cell) [20,21]; (b) BNCT molecules ought to have tumor targeting ability so that the tumor-to-blood boron ratio can be reached high enough to cause damages in tumor cells but leave nearby normal cells un-injured upon neutron irradiation; (c) it has to be able to use MRI to identify the location (or distribution) of the medicinal molecules, since patients cannot be sacrificed, like experimental animals, for measurement of the boron distribution in various organs/tissues.

In literature, HeLa cells are commonly adopted to examine the efficacies of anti-cancer drugs. It was reported that tumor cells are over-expressed with folate receptors on cell membrane, whereas normal cells have very few or none folate receptors [22,23]. Therefore, folate moieties can be used to enhance the cellular uptake efficiency of neutron capture elements-containing molecules or nanomaterials by chemically attaching folate to these molecules or nanomaterials. To conquer the above mentioned challenges and to evaluate the feasibility of neutron capture therapy, we prepare BCo@CNPs, GdCo@CNPs and Co@CNPs as cargoes for neutron capture elements, measure the cytotoxicities of these nanoparticles in HeLa cells, and investigate the cell-killing efficacies upon thermal neurtron irradiation.

2. Materials and methods

2.1. Production of BCo@CNPs, GdCo@CNPs and Co@CNPs

Neutron capture elements-containing carbon nanoparticles were produced by a homemade pulsed DC arc discharge facility. The setup of the device is similar to the conventional Krätschmer–Huffman arc discharge facility; except that the power was supplied by a DC power supplier and the pulse duration was controlled by a wave function generator (see Scheme 1). The anode was a graphite electrode filled with a mixture of boron and cobalt oxide (1:1 mol ratio), gadolinium oxide and cobalt oxide (1:1 mol ratio) or cobalt oxide. The cathode was a tungsten electrode. The bias voltage between the cathode and the anode is 30 V; the pulse duration for electric arcing is 0.2 ms; and the relaxation time between two pulses is also 0.2 ms. The pressure in the arc discharge chamber is 500 Torr Ar atmosphere.

2.2. Procedure for surface grafting of carbon nanoparticles with poly(acrylic acid)

The procedure for surface grafting of carbon nanoparticles is similar to the literature procedures [24,25]. Briefly, 30 mg of carbon nanoparticles and 1 mL of acrylic acid were dispersed homogeneously in 7 mL de-ionized water by ultrasonication. 20 mg of benzoyl peroxide in 0.2 mL THF was injected into the above carbon nanoparticle solution, followed by 1 min sonication and 15 s microwave irradiation in a domestic microwave oven (2.45 GHz, 600 W). The above addition of benzoyl peroxide-sonication-microwave irradiation process was repeated 2–4 times. When the extent of polymerization of acrylic acid becomes higher, the solution becomes more viscous, and so does the extent of surface grafting on carbon nanoparticles. Finally, the surface modified carbon nanoparticles was separated from the free polymer (in the solution) by centrifugation at the speed of 16,000 rpm, and washed with DI water a few times.

2.3. Synthesis of NH_2–PEG–folate [26]

500 mg of polyoxyethylene bis-amine (NH_2–PEG–NH_2, Sigma) was mixed with equal moles of folic acid, N,N′-dicyclohexylcarbodiimide (DCC, TCI) and N-hydroxysuccinimide (NHS, Aldrich) in 5 mL dimethyl sulfoxide (DMSO) in the presence of 10 μL pyridine. The flask was wrapped with aluminum foil (to avoid room light irradiation and subsequent deactivation of folic acid), and sonicated in a water bath for 5 min. The solution was stirred at room temperature overnight under a N_2 atmosphere. The side product, dicyclohexylurea, was removed from the solution by addition of 10 mL water and centrifugation to remove the bottom water layer. The orange color final product, NH_2–PEG–folate, was obtained by rotary evaporation of the remaining solvent.

2.4. Coupling of PAA-grafted carbon nanoparticles and NH_2–PEG–folate

40 mg PAA-grafted carbon nanoparticles, 22.9 mg DCC and 31.9 mg NHS were mixed and dispersed in 7 mL DMSO–pyridine (5:2 v/v) solution. The solution was stirred at room temperature in a N_2 atmosphere for 2 h. The folate–PEG–PAA-grafted carbon nanoparticles were collected by filtration via a filter membrane with pore size of 0.45 μm and washed by THF a few times to remove Dicyclohexylurea, and re-dispersed in 5 mL DMSO. To the solution was added 210 mg NH_2–PEG–folate. The solution was stirred at room temperature in a N_2 atmosphere for 6 h. The final nanoparticle coupling product was collected by an external magnet and washed by THF and methanol a few times to remove physically absorbed NH_2–PEG–folate.

2.5. Cytotoxicity measurements of carbon nanoparticles

To a 24-well plate, it was loaded 1.25×10^4 cells in each well using PBS buffer containing Dulbecco's Modified Eagle Medium (DMEM). Then the plate was incubated for 24 h to allow HeLa cells to stick onto the bottom of the plate and grow. Then, 20 μL of PBS buffer solution containing different amount of carbon nanoparticles (ranging from 100 to 0.09766 μg/mL) was added to the wells, followed by 24 h incubation. To each well, it was added 10 μL of 3-(4,5-Dimethylthiazol-2-yl)-2,5-diphenyltetrazolium bromide (MTT, 5 mg/mL in PBS solution), and the cells were incubated for another 4 h at 37 °C before complete removal of cell solution and addition of 1 mL DMSO to lyses the cells and dissolve the purple formazan product. The cell solution was stirred by pipet to make the purple color homogeneously. The solution was put in an eppendorff, and centrifuged at 13,000 rpm for 10 min. 200 μL of the supernatant was removed and put in another 96-well plate for optical density measurements. The optical density of each well was determined at 570 nm and compared to the standard curve to convert the optical density to equivalent number of cells, and the percentage of cell viabilities.

2.6. Thermal neutron irradiation experiments

In the central 16 wells of a 96-well plate, it was loaded 200 μL of DMEM medium solution containing 1.25×10^4 cells, followed by addition of 20 μL of a PBS buffer solution containing 0.09766 μg of carbon nanoparticles. The plate was put back to an incubator at 37 °C to incubate 24 h and allow HeLa cells to intake carbon nanoparticles. The free carbon nanoparticles in the solution were removed by washing the cells twice using a PBS buffer solution. The plate was then irradiated by a slow thermal neutron beam from the nuclear reactor located inside the campus of National Tsing Hua University, Hsinchu, Taiwan, for 10, 20, and 40 min. After neutron irradiation, the plates were further incubated at 37 °C for 8, 24, and 48 h, and then

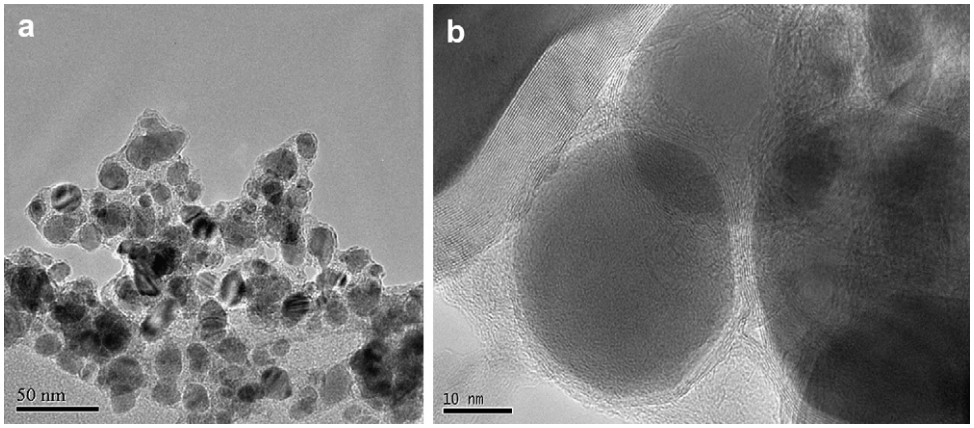

Fig. 1. (a) Low resolution TEM image of as-produced BCo@CNPs carbon soots. (b) High resolution TEM image of BCo@CNPs.

cell viabilities were determined. The cell viabilities of HeLa cells fed with carbon nanoparticles after neutron irradiation were obtained by normalization to that without being fed with carbon nanoparticles but receiving the same amount of neutron irradiation dose. Control experiments show that For HeLa cells without being fed with carbon nanoparticles, the cell viabilities did not show any noticeable differences whether or not receiving 10 or 20 min neutron irradiation. All data were obtained by average of 2–3 sets of the same experiments.

3. Results and discussion

In the current study, boron and cobalt-containing carbon nanoparticles, BCo@CNPs, were produced by a homemade, modified DC pulsed arc process (see the experimental section for details). In conventional electric arc discharge processes, carbon nanoparticles were produced as a minor product, in addition to carbon nanotubes and amorphous carbon species. It is quite difficult to produce carbon nanoparticles as the major product without co-existence of carbon nanotubes. Due to the smaller sizes, carbon nanoparticles are much easier for cells to uptake than long carbon nanotubes. Many efforts have been devoted to searching for processes to produce carbon nanoparticles with well graphitized carbon shells as the major products. However, only limited numbers of processes are successful [27–30]. As shown in Fig. 1(a), transmission electron microscope (TEM) image shows that most of the as-produced carbon soots are spherical nanoparticles with sizes in the range of 20–50 nm (see Fig. 1(a)), in addition to some amorphous carbon species. Almost no carbon nanotubes were produced in this pulsed DC arc discharge process. High resolution TEM image shows that BCo@CNPs has well-defined graphene layers with cobalt nanoparticles encapsulated in the central core of the nanoparticle (see Fig. 1(b)). XRD measurement of BCo@CNCs show that the encapsulated Co nanoparticle is present in the form of CoB alloy (see Supplementary Figure S1). Mapping of electron energy loss spectra (EELS) shows that the boron atoms are evenly distributed in the whole carbon nanoparticle; and cobalt nanoparticle was encapsulated in the central core of carbon shells (see Supplementary Figure S2). From the intensity ratio of the electron energy loss signals of the boron and carbon K shell electrons, the atomic ratio of boron to carbon was estimated to be ~1/10, whereas the B to Co ratio in the BCo@CNCs was measured by inductively coupled plasma-atomic emission spectrum (ICP-AES) to be 1:1.54. Overall, the atomic ratio among B:Co:C is around 1:1.54:10, i.e., the molar percentage of boron in the BCo@CNPs is ~8% (or ~1.6% ^{10}B isotope). By a similar way, gadolinium-cobalt-containing carbon nanoparticles (GdCo@CNPs) were also prepared. Similar to the BCo@CNPs, GdCo@CNPs also has clear and well-defined graphene layers (see Figure S3(a) & (b) for low and high resolution TEM images, respectively). Powder X-ray diffraction (XRD) measurement of the GdCo@CNPs shows that most of Gd-atoms exist in the form of Gd_2C_3 carbide (see Supplementary Figure S4), instead of GdCo alloy; whereas, the Co element is present in the form of face centered cubic crystalline structure. It is commonly observed that lanthanide elements prefer to form metal carbides, rather than to exist in a pure metallic form [27,31,32]. It has been proven difficult to prepare GdCo@CNPs having encapsulated GdCo alloy [31,32]. For the purpose of neutron capture therapy, it does not matter whether the Gd element exists as a GdCo alloy or as a Gd carbide. However, for the purpose of magnetic resonance imaging (MRI), it is better to have GdCo alloy, since metal alloy usually has a larger saturation magnetization value than their corresponding carbides [33]. From both the

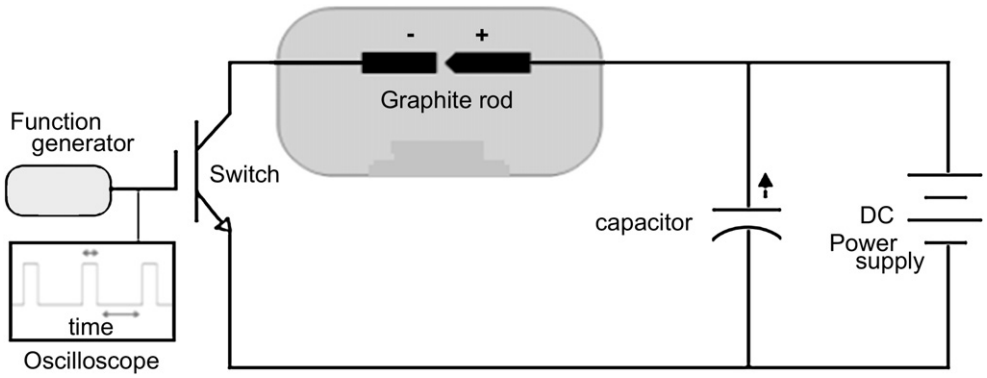

Scheme 1. The Schematic setup for the DC pulsed electric arc discharge facility for production of neutron capture element-containing carbon nanoparticles.

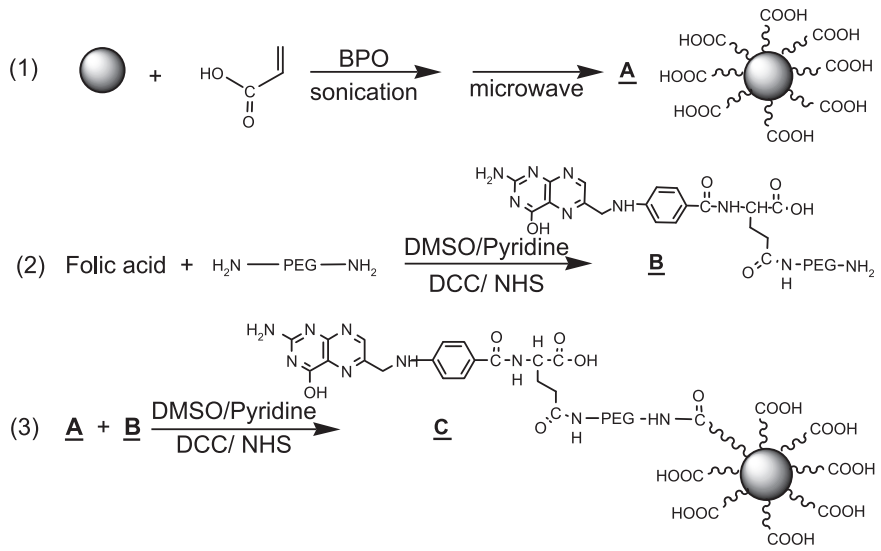

Scheme 2. Reaction steps for surface functionalization of BCo@CNPs, GdCo@CNPs and Co@CNPs with folate moieties. In step (1), carbon nanoparticles were surface grafted with poly(acrylic acid) (PAA) by a sonication-microwave method. In step (2), the terminal carboxylic acid moiety of folic acid was coupled to polyoxyethylene bis-amine using DCC/NHS reagents in DMSO-pyridine co-sovlent, and then further coupled to the PAA-grafted carbon nanoparticles in step (3), where DCC is N,N′-dicyclohexylcarbodiimide, and NHS is N-hydroxysuccinimide.

intensity ratio of EELS and ICP-AES measurements, the Gd:Co:C ratios were determined to be 1:11.43:10; that is, the molar percentage of Gd is about 4.4 mol%. Superconducting quantum interference devices (SQUID) measurements show that the saturation magnetization values of BCo@CNPs, GdCo@CNPs, and Co@CNPs are 1, 8, and 30 emu/g, respectively (see Supplementary Figure S5). The Co@CNPs was prepared in the similar way as those of BCo@CNPs and GdCo@CNPs, except that cobalt oxide was used in the DC pulsed arc discharge process, rather than boron-cobalt oxide or gadolinium oxide-cobalt oxide mixture. High resolution TEM image shows that the Co@CNPs, similar to the other two CNPs, has an fcc-Co nanoparticle being wrapped by well graphitized graphene layers (see Supplementary Figure S6 for TEM images and Figure S7 for XRD spectrum).

For cellular experiments, carbon nanoparticles were surface functionalized with poly(acrylic acid) (PAA) to become soluble in water [24,25], followed by coupling to NH_2–PEG–folate, where PEG represents polyoxyethylene. The NH_2–PEG–folate was pre-synthesized via coupling of folic acid and polyoxyethylene bis-amine together. The synthetic procedures were shown in Scheme 2. The final carbon nanoparticles bear folate moieties, and are able to bind to folate receptors on HeLa tumor cells. The attachment of folate moieties on carbon nanoparticles could enhance the uptake of nanomaterials via receptor-mediated endocytosis process [34,35]. Previously, it was also observed that attachment of folate to lipid molecules enhances liposome binding to tumor cells [36]. Fig. 2 shows the FT-IR spectra of PAA-grafted, PEG–PAA-grafted and folate–PEG–PAA-grafted BCo@CNPs. The FT-IR spectrum in Fig. 2(a) shows the characteristic stretching peaks of O–H bond and >C=O bond of the acrylic acid moieties of PAA at ~3450 and 1730 cm^{-1}, respectively. Upon being coupled with polyoxyethylene bis-amine (NH_2–PEG–NH_2), the >C=O of the acrylic acid moieties was converted to peptide –N(H)C=O bond, which is evidenced by shift of the 1730 cm^{-1} band to 1632 cm^{-1}, in accompanied with the occurring of

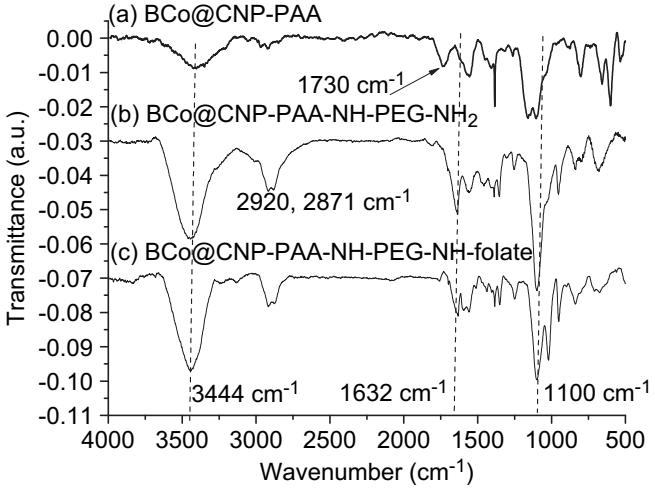

Fig. 2. FT-IR spectra of (a) PAA-grafted, (b) NH_2–PEG–PAA-grafted, and (c) folate–PEG–PAA-grafted BCo@CNPs.

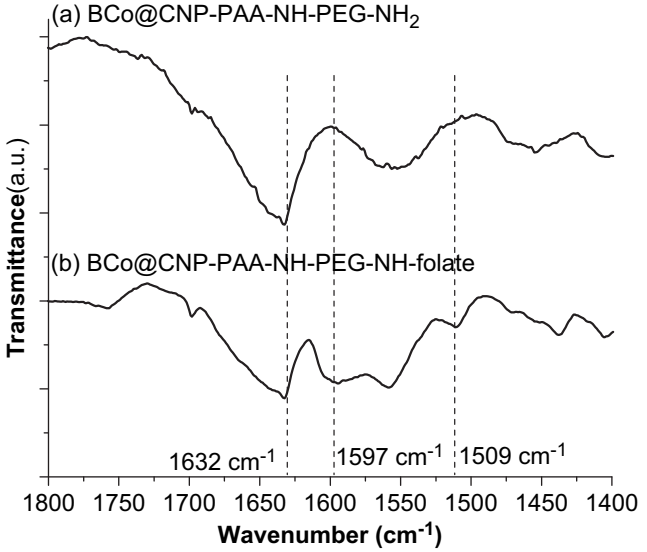

Fig. 3. Enlarged FT-IR spectra of Fig. 2(b) and (c) in the range of 1400–1800 cm^{-1} for NH_2–PEG–PAA-grafted, and folate–PEG–PAA-grafted BCo@CNPs.

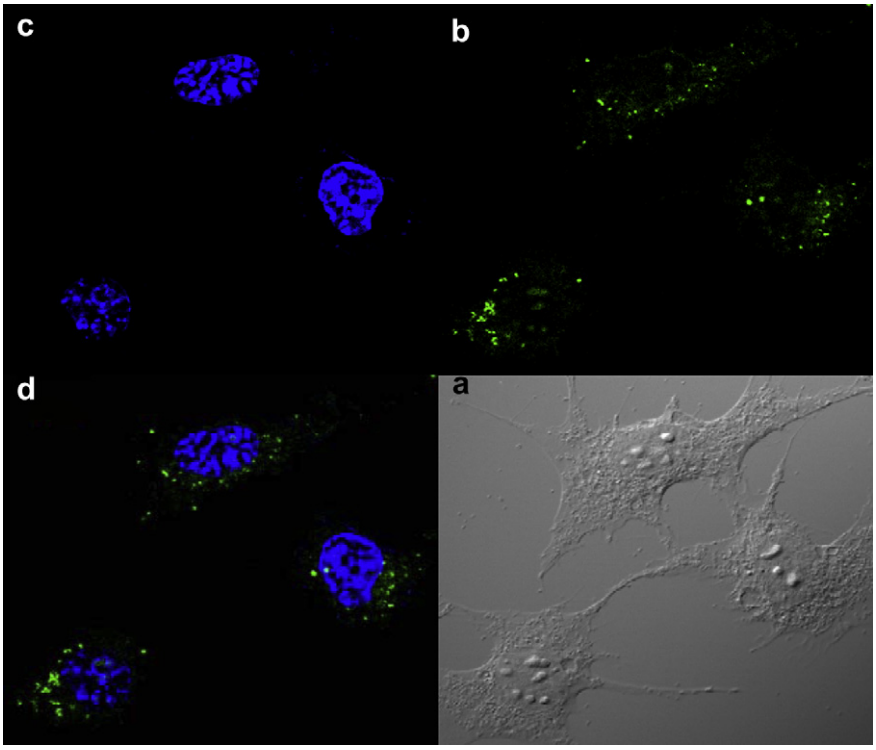

Fig. 4. Vertical cross-section optical images of HeLa cells. The image in (a) is a visible light optical image of HeLa cells fed with BCo@CNPs–PAA–folate with a dose of 0.09677 μg/mL. (b) The green fluorescence was from the folate moieties on BCo@CNPs–PAA–folate under a FITC filter (λ_{ex} = 478–495 nm, λ_{em} = 510–550 nm). (c) The nuclei of HeLa cells were stained with a DAPI (blue) dye. The image was taken using a DAPI filter (λ_{ex} = 400–414 nm, λ_{em} = 450–465 nm). (d) The optical image in (d) was an overlay image of (b) and (c).

the strong ether C–O stretching band at ~1100 cm^{-1} (see Fig. 2(b)). The bands at 2920 and 2871 cm^{-1} are due to the C–H stretching signal from the PEG moieties. As compared to Fig. 2(a), the strong, broad band at 3450 cm^{-1} is most probably due to overlapping of the terminal amino NH_2 and peptide –NH–(C=O) moieties in the PEG chains. When PAA-grafted BCo@CNPs was directly coupled to NH_2–PEG–folate, instead of NH_2–PEG–NH_2, the FT-IR spectrum looks very similar, but slightly different from that shown in Fig. 2(b) (see Fig. 2(c) vs. Fig. 2(b)). The major difference occurs in the region between 1700 and 1400 cm^{-1} region, which was enlarged in Fig. 3. The stretching signal from the >C=O in the peptide (–NHC=O) moieties remains the same at ~1632 cm^{-1}. The additional weak bands at ~1597 and ~1509 cm^{-1} were attributed to the aromatic C=C bending bands of the folate moieties (see Fig. 3).

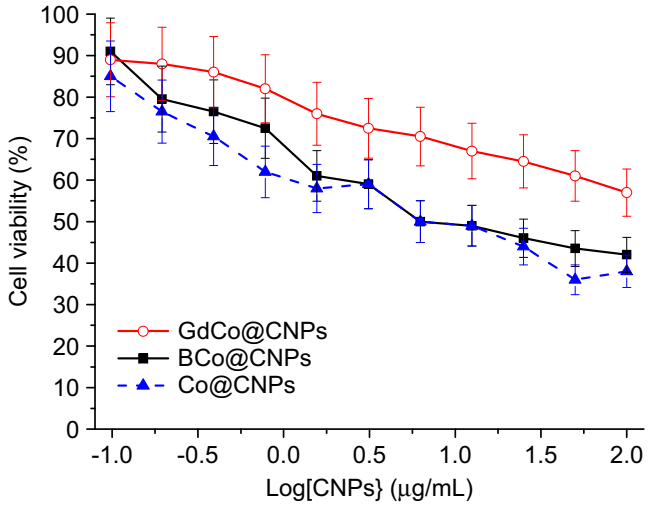

Fig. 5. Cell viabilities of HeLa cells as a function of doses of different carbon nanoparticles, including BCo@CNPs (■), GdCo@CNPs (○) and Co@CNPs (▲).

To examine whether these carbon nanoparticles have neutron capture therapeutic (NCT) effects, in vitro cellular experiments were conducted using HeLa cells. Fig. 4 shows the confocal optical images of HeLa cells fed with folate-grafted BCo@CNPs. The green fluorescence was from the folate moieties. The confocal optical images show that upon internalization, nanoparticles stay in the cytoplasm without entering the nucleus which was stained by a blue fluorescent dye, 4′,6-diamidino-2-phenylindole (DAPI). Fig. 5 shows the cytotoxicities of these three nanoparticles as a function of nanoparticle doses. The IC_{50}s of BCo@CNPs, GdCo@CNPs and Co@CNPs are about 6.25, 6.25, and >200 μg/mL, respectively. For thermal neutron irradiation experiments, the dose of nanoparticles was chosen to be 0.09677 μg/ml, where the cytotoxicities are low and the cell viabilities of HeLa cells are 91%, 89%, and 85% for folate-grafted BCo@CNPs, GdCo@CNPs and Co@CNPs, respectively. The neutron source was from the Nuclear Reactor located in the campus of National Tsing Hua University, Hsinchu, Taiwan. The cell viabilities were obtained using the MTT (3-(4,5-Dimethyl thiazol-2-yl)-2,5-diphenyltetrazolium bromide) assay, of which the optical densities were normalized to the control set of experiments where the HeLa cells received the same amount of neutron dose but without being fed with carbon nanoparticles. As shown in Fig. 6(a), HeLa cells fed with BCo@CNPs, GdCo@CNPs, and Co@CNPs have cell viabilities of ~48, ~45, and ~72%, respectively, at 8 h after thermal neutron irradiation with a dose of 6×10^{11} n/cm^2 (or 10 min irradiation with a neutron beam intensity of 1×10^9 n/cm^2 s). In other words, 10 min thermal neutron irradiation causes acute cell deaths of 52, 55, and 28% for HeLa cells fed with BCo@CNPs, GdCo@CNPs, and Co@CNPs, respectively, at 8 h after irradiation. The results demonstrate that these neutron capture elements-containing carbon nanoparticles

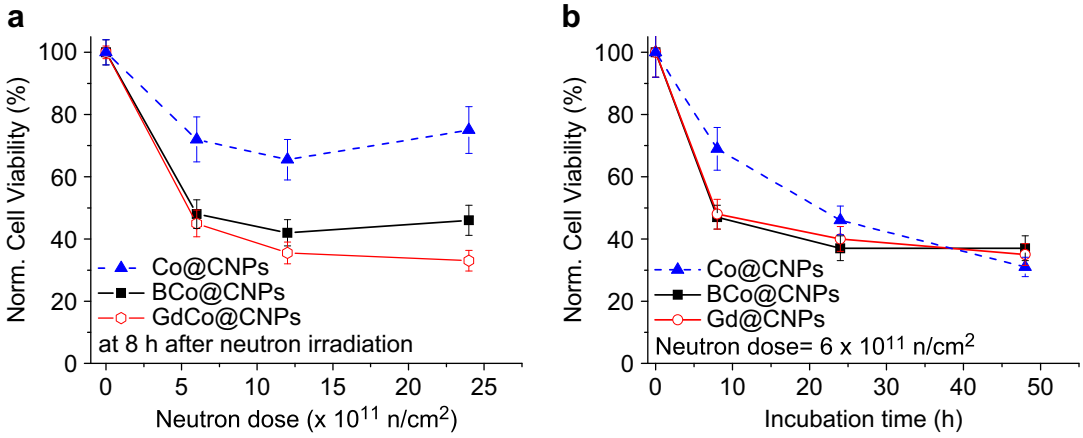

Fig. 6. (a) Normalized cell viabilities of HeLa cells as a function of the neutron irradiation dose. The HeLa cells were fed with different M@CNPs (M = BCo, GdCo, and Co). The cell viabilities were measured at 8 h after neutron irradiation. (b) Normalized cell viabilities of HeLa cells fed with different M@CNPs as a function of time after neutron irradiation with a dose of 6×10^{11} n/cm^2. All cell viabilities were normalized to the control set of HeLa cells without being fed with M@CNPs but receiving the same amount of neutron doses.

are very promising NCT nanomaterials, and are probably far better than the 1st and 2nd generations of B or Gd-atom based NCT molecules, since a B- or Gd-containing carbon nanoparticle can carry hundred or thousand times more neutron capture elements than the previous molecule-based counter parts. Double or quadruple the neutron irradiation doses only leads to slight variation in the cell viability (or acute cell death rates), which might be due to nearly complete consumption of neutron capture elements during the first 10 min irradiation (see Fig. 6(a)). To examine whether the proliferation capabilities of survived HeLa cells were affected by the NCT treatments, the cell viabilities were measured as a function of the incubation time for HeLa cells receiving 10 min thermal neutron irradiation. As shown in Fig. 6(b), the cell viabilities of HeLa cells fed with nanoparticles continue dropping at 24 and 48 h after 10 min neutron irradiation, indicating that the survived HeLa cells, albeit still surviving, are damaged by the NCT treatment and their proliferation capabilities decline as compared to the control set of HeLa cells receiving the same amount of neutron dose but without being fed with nanoparticles. Upon absorption of neutrons, Gd-atoms become radioactive, and decay immediately to generate γ-ray and a high energy Auger–Coster–Kronig electron with 7.94 MeV energy [37,38]. The Auger–Coster–Kronig electron has a very short mean free path length of a few nanometers, and is very effective in destroying DNA [39]. Since Gd is also a magnetic nucleus, molecules containing Gd not only can serve as a thermal neutron capture therapy reagent, but also act as an MRI contrast reagent [40,41]. ^{59}Co atom, similar to ^{10}B and Gd, has a thermal neutron capture cross-section of 1900 b [3], and can be converted to become radioactive ^{60}Co upon receiving neutron irradiation. Radioactive ^{60}Co has a half-life of 5.26 years and decays by emitting a beta ray (an electron) to excited state ^{60}Ni, which then further decays immediately to ground state ^{60}Ni and emits two gamma decays with energy of 1.17 and 1.33 MeV, respectively [42]. Therefore, Co@CNPs also has weak neutron capture therapeutic effect and causes ~28% the acute cell death as compared to the other two nanoparticles (see Fig. 5(a)). Fig. 6(b) shows that Co@CNPs has more pronounced long term damage effect on the proliferation capability of survived HeLa cells than the other two nanoparticles.

4. Conclusion

In summary, we have demonstrated "proof-of-concept" examples for BNCT, Gd-NCT, and Co-NCT at the cell level that ^{10}B, ^{157}Gd and ^{59}Co-containing carbon nanoparticles indeed can effectively induce acute cell deaths upon receiving thermal neutron irradiation. These carbon nanoparticles were surface modified with folate moieties, and therefore, are able to target tumor cells having folate receptors over-expressed on cell membrane. 10 min irradiation with a neutron intensity of 1×10^9 n/cm^2 s results in 52, 55, and 28% acute cell death for HeLa cells fed with BCo@CNPs, GdCo@CNPs, and Co@CNPs, respectively, at 8 h after neutron irradiation. After thermal neutron irradiation, the proliferation capability of survived HeLa cells was also found to be significantly suppressed as compared to the control set of HeLa cells which received the same amount of neutron dose but without internalization of nanoparticles. The medicinal efficacies of these carbon nanoparticles can be further optimized using pure ^{10}B or ^{157}Gd isotopes, or by increasing larger percentages of neutron capture elements in the precursors for preparation of carbon nanoparticles. Since these nanomaterials are also magnetic, they have great potential to serve as both diagnostic MR imaging probes and therapeutic drugs simultaneously. Due to its compact structure, a single carbon nanoparticle can carry hundreds or thousands times more neutron capture atoms than a molecule-based counterpart. Our results clearly demonstrate that these neutron capture elements-containing nanoparticles are very promising medicinal nanomaterials for NCT destruction of cancers/tumors and potentially for diagnosis as well.

Acknowledgement

The authors are grateful to the financial support from the National Science Council, Taiwan.

Appendix. Supplementary data

Supplementary data associated with this article can be found in the on-line version, at doi:10.1016/j.biomaterials.2010.07.057.

Appendix

Figures with essential color discrimination. Figs. 5 and 6 in this article are difficult to interpret in black and white. The full color images can be found in the on-line version, at doi:10.1016/j.biomaterials.2010.07.057.

References

[1] Locher GL. Biological effects and therapeutic possibilities of neutrons. Am J Roentgenol Radium Ther 1936;36:1–13.
[2] Coderre JA, Morris GM. The radiation biology of boron neutron capture therapy. Radiat Res 1999;151(1):1–18.
[3] Soloway AH, Tjarks W, Barnum BA, Ron FG, Barth RF, Codogni IM, et al. The chemistry of neutron capture therapy. Chem Rev 1998;98(4):1515–62.
[4] Godwin JT, Farr LE, Sweet WH, Robertson JS. Pathological study of 8 patients with glioblastoma multiforme treated by neutron-capture therapy using boron-10. Cancer 1955;8(3):601–15.
[5] Hawthorne MF, Lee MW. A critical assessment of boron target compounds for boron neutron capture therapy. J Neurooncol 2003;62(1):33–45.
[6] Coderre JA, Elowitz EH, Chadha M, Bergland R, Capala J, Joel DD, et al. Boron neutron capture therapy for glioblastoma multiforme using p-boronophenylalanine and epithermal neutrons: trial design and early clinical results. J Neurooncol 1997;33(1–2):141–52.
[7] Neumann M, Bergmann M, Gabel D. Cell type selective accumulation of mercaptoundecahydro-closo-dodecaborate (BSH) in glioblastoma multiforme. Acta Neurochir 2003;145(11):971–5.
[8] Braun K, Wolber G, Waldeck W, Pipkorn R, Jenne J, Rastert R, et al. The enhancement of neutron irradiation of HeLa-S cervix carcinoma cells by cell-nucleus-addressed deca-p-boronophenylalanine. Eur J Med Chem 2003;38(6):587–95.
[9] Kane RR, Drechsel K, Hawthorne MF. Automated syntheses of carborane-derived homogeneous oligophosphates-reagents for use in the immunoprotein-mediated boron neutron-capture therapy (BNCT) of cancer. J Am Chem Soc 1993;115(19):8853–4.
[10] Yinghuai Z, Peng AT, Carpenter K, Maguire JA, Hosmane NS, Takagaki M. Substituted carborane-appended water-soluble single-wall carbon nanotubes: new approach to boron neutron capture therapy drug delivery. J Am Chem Soc 2005;127(27):9875–80.
[11] Mortensen MW, Bjorkdahl O, Sorensen PO, Hansen T, Jensen MR, Gundersen HJG, et al. Functionalization and cellular uptake of boron carbide nanoparticles: the first step toward T cell-guided boron neutron capture therapy. Bioconjug Chem 2006;17(2):284–90.
[12] van Rij CM, Wilhelm AJ, Sauerwein WAG, van Loenen AC. Boron neutron capture therapy for glioblastoma multiforme. Pharm World Sci 2005;27(2):92–5.
[13] El-Zaria ME, Ban HS, Nakamura H. Boron-containing protoporphyrin IX derivatives and their modification for boron neutron capture therapy: synthesis, characterization, and comparative in vitro toxicity evaluation. Chem Eur J 2010;16(5):1543–52.
[14] Li T, Hamdi J, Hawthorne MF. Unilamellar liposomes with enhanced boron content. Bioconjug Chem 2006;17(1):15–20.
[15] Ueno M, Ban HS, Nakai K, Inomat R, Kaneda Y, Matsumura A, et al. Dodecaborate lipid liposomes as new vehicles for boron delivery system of neutron capture therapy. Bioorg Med Chem 2010;18(9):3059–65.
[16] Nigg DW. Computational dosimetry and treatment planning considerations for neutron capture therapy. J Neurooncol 2003;62(1):75–86.
[17] Pantarotto D, Singh R, McCarthy D, Erhardt M, Briand JP, Prato M, et al. Functionalized carbon nanotubes for plasmid DNA gene delivery. Angew Chem Int Ed 2004;43(39):5242–6.
[18] Kam NWS, Liu Z, Dai HJ. Carbon nanotubes as intracellular transporters for proteins and DNA: an investigation of the uptake mechanism and pathway. Angew Chem Int Ed 2006;45(4):577–81.
[19] Liu Z, Cai W, He L, Nakayama N, Chen K, Sun X, et al. In vivo biodistribution and highly efficient tumour targeting of carbon nanotubes in mice. Nat Nanotech 2007;2(1):47–52.
[20] Javid M, Brownell GL, Sweet WH. The possible use of neutron-capturing isotopes such as boron-10 in the treatment of neoplasms 2. computation of the radiation energies and estimates of effects in normal and neoplastic brain. J Clin Invest 1952;31(6):604–10.
[21] Tolpin EI, Wellum GR, Dohan Jr FC, Kornblith PL, Zamenhof RG. Boron neutron-capture therapy of cerebral gliomas 2. Utilization of blood–brain-barrier and tumor-specific antigens for selective concentration of boron in gliomas. Oncology 1975;32(5–6):223–46.
[22] Elnakat H, Ratnam M. Distribution, functionality and gene regulation of folate receptor isoforms: implications in targeted therapy. Adv Drug Deliv Rev 2004;56(8):1067–84.
[23] Ross JF, Chaudhuri PK, Ratnam M. Differential regulation of folate receptor isoforms in normal and malignant-tissures in-vivo and in established cell-lines-physiological and clinical implications. Cancer 1994;73(9):2432–43.
[24] Hsin YL, Lai JY, Hwang KC, Lo SC, Chen FR, Kai JJ. Rapid surface functionalization of iron-filled multi-walled carbon nanotubes. Carbon 2006;44(15):3328–35.
[25] Chang IP, Hwang KC, Ho JAA, Lin CC, Hwu RJR, Horng JC. Facile surface functionalization of nanodiamonds. Langmuir 2010;26(5):3685–9.
[26] Lee RJ, Low PS. Folate-mediated tumor-cell targeting of liposome-entrapped doxorubicin in-vitro. Biochim Biophys Acta 1995;1233(2):134–44.
[27] Hwang KC. Recent progress in the preparation and applications of carbon nanoocapsules. J Phys D Appl Phys, in press.
[28] Dravid VP, Host JJ, Teng MH, Elliott B, Hwang J, Johnson DL, et al. Controlled-size nanocapsules. Nature 1995;374(6523):602.
[29] Liang YC, Hwang KC, Lo S-C. Solid-state microwave-arcing-induced formation and surface functionalization of core/shell metal/carbon nanoparticles. Small 2008;4(4):405–9.
[30] Hsin YL, Lin CF, Liang YC, Hwang KC, Horng JC, Ho JAA, et al. Microwave arcing induced formation and growth mechanisms of core/shell metal/-carbon nanoparticles in organic solutions. Adv Funct Mater 2008;18(14):2048–56.
[31] Saito Y. Nanoparticles and filled nanocapsules. Carbon 1995;33(7):979–88.
[32] Saito Y, Okuda M, Yoshikawa T, Kasuya A, Nishina Y. Correlation between volatility of rare-earth-metals and encapsulation of their carbides in carbon nanocapsules. J Phys Chem 1994;98(27):6696–8.
[33] Diggs B, Zhou A, Silva C, Kirkpatrick S, Nuhfer NT, McHenry ME, et al. Magnetic-properties of carbon-coated rare-earth carbide nanocrystallites produced by a carbon-arc method. J Appl Phys 1994;75(10):5879–81.
[34] Anderson RGW, Kamen BA. Potocytosis-sequestration and transport of small molecules by caveolae. Science 1992;255(5043):410–1.
[35] Goren D, Horowitz AT, Tzemach D, Tarshish M, Zalipsky S, Gabizon A. Nuclear delivery of doxorubicin via folate-targeted liposomes with bypass of multi-drug-resistance efflux pump. Clin Cancer Res 2000;6(5):1949–57.
[36] Gabizon A, Horowitz AT, Goren D, Tzemach D, Mandelbaum-Shavit F, Qazen MM, et al. Targeting folate receptor with folate linked to extremities of poly(ethylene glycol)-grafted liposomes: in vitro studies. Bioconjug Chem 1999;10(2):289–98.
[37] Salt C, Lennox AJ, Takagaki M, Maguire JA, Hosmane NS. Boron and gadolinium neutron capture therapy. Russ Chem Bull 2004;53(9):1871–88.
[38] Shih JLA, Brugger RM. Gadolinium as a neutron-capture therapy agent. Med Phys 1992;19(3):733–44.
[39] Goorley T, Zamenhof R, Nikjoo H. Calculated DNA damage from gadolinium auger electrons and relation to dose distributions in a head phantom. Int J Radiat Biol 2004;80(11–12):933–40.
[40] Flacke S, Fischer S, Scott MJ, Fuhrhop RJ, Allen JS, McLean M, et al. Novel MRI contrast agent for molecular imaging of fibrin implications for detecting vulnerable plaques. Circulation 2001;104(11):1280–5.
[41] Gupta AK, Gupta M. Synthesis and surface engineering of iron oxide nanoparticles for biomedical applications. Biomaterials 2005;26(18):3995–4021.
[42] Weiss HV, Shipman WH. Biological concentration by killer clams of cobalt-60 from radioactive fallout. Science 1957;125(3250):695.